3D extrusion printing of high drug loading immediate release paracetamol tablets

Shaban A Khaled[a], Morgan R. Alexander[a], Ricky D. Wildman[b], Martin J. Wallace[c], Sonja Sharpe[d], Jae Yoo[d] and Clive J. Roberts[a*]

[a] Advanced Materials and Healthcare Technologies, School of Pharmacy, The University of Nottingham, Nottingham, NG7 2RD, UK

[b] EPSRC Centre for Innovative Manufacturing in Additive Manufacturing, School of Engineering, UK

[c] Advanced Manufacturing Technology, GlaxoSmithKline (Ireland), 12 Riverwalk, Citywest, Business Campus, Dublin, 24, Ireland

[d] Advanced Manufacturing Technology, GlaxoSmithKline, 709 Swedeland Rd., King of Prussia, PA 19406-0939, USA

[*]Correspondence to: Clive J Roberts

Address: School of Pharmacy, The University of Nottingham, University Park, NG7 2RD, UK

Tel: +44 115 951 5048
Fax: +44 115 951 5102
Email: clive.roberts@nottingham.ac.uk

Abstract

The manufacture of immediate release high drug loading paracetamol oral tablets was achieved using an extrusion based 3D printer from a premixed water based paste formulation. The 3D printed tablets demonstrate that a very high drug (paracetamol) loading formulation (80% w/w) can be printed as an acceptable tablet using a method suitable for personalisation and distributed manufacture. Paracetamol is an example of a drug whose physical form can present challenges to traditional powder compression tableting. Printing avoids these issues and facilitates the relatively high drug loading.

The 3D printed tablets were evaluated for physical and mechanical properties including weight variation, friability, breaking force, disintegration time, and dimensions and were within acceptable range as defined by the international standards stated in the United States Pharmacopoeia (USP). X-Ray Powder Diffraction (XRPD) was used to identify the physical form of the active. Additionally, XRPD, Attenuated Total Reflectance Fourier Transform Infrared spectroscopy (ATR-FTIR) and differential scanning calorimetry (DSC) were used to assess possible drug-excipient interactions. The 3D printed tablets were evaluated for drug release using a USP dissolution testing type I apparatus. The tablets showed a profile characteristic of the immediate release profile as intended based upon the active/excipient ratio used with disintegration in less than 60 seconds and release of most of the drug within 5 minutes. The results demonstrate the capability of 3D extrusion based printing to produce acceptable high-drug loading tablets from approved materials that comply with current USP standards.

1.1. Introduction

Paracetamol is available in many different dosage forms including tablets, capsules, suspensions, suppositories and intravenous solutions and is commonly used to alleviate mild to moderate pain caused by headaches, toothache, sprain, or strains (Whittaker, 2011). It is usually used in oral solid dosage forms in an active dose range from 300-500 mg, although 1000 mg is also available in some regions. Direct compression is the most common method used for tableting production (Gohel and Jogani, 2005), as it is a relatively straightforward process compared with other tablet manufacturing process such as wet granulation. However, direct compression is limited to relatively low drug loading tablet production due to the mechanical properties of some actives, including paracetamol, compromising compression characteristics. Poorly compressible active ingredients mean that only 30-40 % w/w of the active can be accommodated and therefore, production of 500 mg paracetamol tablets requires compression of a formulation with a final weight of 1300 mg including 800 mg of excipients. This can cause patient non-compliance due to the large tablets being difficult to swallow or even to choking (Gohel and Jogani, 2005, Govedarica et al., 2009, Kaerger et al., 2004). Segregation of powder constituents and dust contamination are another problems in the direct compression process (Gohel and Jogani, 2005). This can be addressed by granulation, a process well known in the manufacturing of paracetamol tablets. This process, however, also has some limitations compared with extrusion based 3D printing process. These include; lower paracetamol loading leading to a higher final product total weight, material loss during the various stages of processing and multiple processing steps adding complexity (Agrawal and Naveen, 2011). This could in general make 3D printing an attractive way of manufacturing tablets using inexpensive single step.

Paracetamol exists in three different polymorphs; forms I, II, and III; exhibiting different free energies and different physicochemical properties such as melting point, stability, dissolution

82 rate, deformation characteristics (affecting compressibility) and crystal shape and size
83 (affecting powder density and flow properties) (Capes and Cameron, 2007, Di Martino et al.,
84 1997, Sibik et al., 2014). Paracetamol form I is preferred in tablet production because it is the
85 most stable form (Nichols and Frampton, 1998). However, the crystals of paracetamol form I
86 display low flowability and a poor compression ability, and when such crystals compressed
87 into tablets they show massive elastic deformation under pressure and a tendency to cause
88 problems with tablets such as chipping, capping, stress cracking, lamination, sticking and
89 picking (Eichie and Amalime, 2007, Govedarica et al., 2009, Karki et al., 2009, Martinello et
90 al., 2006, Ngwuluka et al., 2010, Wu et al., 2008). In order to reduce the above-mentioned
91 problems and improve compressibility, paracetamol tablets are typcially prepared by adding a
92 high quantity of excipients such as starch, carboxymethyl cellulose, pre-gelatinized starch,
93 and gelatine (direct compression) or by the addition of binders (granulation process)
94 (Martinello et al., 2006, Ngwuluka et al., 2010). Each one of these additions can introduce
95 expense and increasing tablet weight and size (Di Martino et al., 1996, Fachaux et al., 1995,
96 Khaled et al., 2014). There is little work on 3D printing of paracetamol formulations in the
97 literature and these are mostly by FDM 3D printing (Goyanes et al., 2017, Goyanes et al.,
98 2016, Wang et al., 2016). However, the high extrusion temperatures applied (≥180 °C) using
99 FDM narrow the active ingredient library that can be used by this process to include only heat
100 stable actives. Also, the print resolution is affected by the drug loading leading to partial loss
101 in the object morphology definition at high loading, and therefore affecting the final product
102 quality (Goyanes et al., 2017)

103 3D printed oral tablets manufactured via different 3D printers have been demonstrated (Clark
104 et al., 2017, Goyanes et al., 2015, Holländer et al., 2016, Kyobula et al., 2017, Rattanakit et
105 al., 2012, Rowe et al., 2000, Skowyra et al., 2015, Sun and Soh, 2015, Wang et al., 2016).
106 Spritam® was the first FDA approved 3D printed medicine manufactured by the

107 pharmaceutical company, Aprecia, in which the active is the anti-epileptic drug
108 levetiracetam. The tablets were printed with high drug loading using a continuous process of
109 spreading a layer of powder onto a movable piston plate, during which the drug/additives
110 particles were bound together to form a solid layer by the spreading of a liquid binder
111 solution. The printing process was repeated continuously until the desired tablet dimension is
112 achieved. This method of printing was also demonstrated by Katstra et al. who showed that
113 problems related to ink bleeding, drug migration, and the capillary effect of the binder on the
114 powder bed (formulation/binder saturation), geometry restrictions and organic solvent
115 residues mean that it is suitable only for a small range of excipients and drugs (Katstra et al.,
116 2000, Rowe et al., 2000, Wang et al., 2016). Drug loading limits and the consequences of
117 printing at high temperature are known issues in other 3D printing methods of tablet
118 production (Gohel and Jogani, 2005, Goyanes et al., 2015) due to ink (printable formulation)
119 rheology and drug degradation in the 3D printing technologies available. This is particularly
120 so for inkjet and fused deposition modelling (FDM) methods, respectively. However, the
121 drug loading of FDM has been reported to be able to reach 50% (Pietrzak et al., 2015).

122 We propose that a paste-based extrusion 3D printing process using standard pharmaceutical
123 excipients will be applicable to a wider range of drugs and excipients and allows higher drug
124 loading (Khaled et al., 2014, Khaled et al., 2015, Khaled et al., 2015). Additional advantages
125 include the avoidance of possible drug degradation caused by the high temperatures and UV
126 irradiation used in FDM and UV-curing based ink-jet methods, respectively (Okwuosa et al.,
127 2016). Furthermore, extrusion is generally a well understood process being used in
128 pharmaceutical and other industries for many years and the materials used in extrusion
129 process already having compendia grades available for pharmaceutical applications.
130 However, extrusion based 3D printing does have a number of disadvantages; relatively coarse

131 resolution compared with inkjet, SLS, and SLA 3D printers, not suitable for humid sensitive
132 materials (degradation) and a risk of phase separation.

133 **1.2. Material and methods**

134 **1.2.1. Materials**

135 Paracetamol, polyvinylpyrrolidine (PVP K25), sodium phosphate monobasic and dibasic
136 were supplied by Sigma–Aldrich (Gillingham, UK). Croscarmellose sodium (CCS)
137 (Primellose®) was kindly supplied as a gift from DFE Pharma. Milli-Q water (resistivity 18.2
138 MΩ cm) was used for all formulations and solutions.

139 **1.2.2. Methods**

140 **1.2.2.1. Design of paracetamol tablets**

141 An oval shaped tablet was chosen as a style of tablet made to be easy to swallow. The 3D
142 tablet was designed to achieve an immediate drug release profile based upon the
143 active/excipient ratio used. The dimension of the designed oval tablet was 14.5 mm length ×
144 7.5 mm width × 4.9 mm height. The number of the printed layers was 14 with a 0.35 mm
145 thickness for each layer. The selected tablet size and shape could improve patient compliance
146 with medication regimen (Brotherman et al., 2004, Channer and Virjee, 1986, Hey et al.,
147 1982). The geometry of the 3D printed tablets was programmed using a 3D drawing package
148 (BioCAD, regenHU Villaz-St-Pierre, Switzerland).

149 **1.2.2.2. Extrusion based 3D printing process of paracetamol tablets**

150 Paracetamol powder was ground using a standard coffee machine to achieve particles less
151 than 100 um diameter (mesh with pores of 100 um diameter was used to sieve ground
152 paracetamol powder). The paracetamol ground powder and the required excipients (CCS and
153 PVP K25) were mixed using a mortar and pestle for 15 min. Two grams of the blend were
154 accurately weighed and mixed to form a paste with 1.3 ml of Milli-Q water (the disintegrant

155 (NaCCS) was responsible for the addition of a high amount of water) according to the
156 formulae shown in Table 1.

157 **1.2.2.3.Cartridge tool filling and 3D printing processes**

158 A plastic 5 cm^3 syringe (Optimum® syringe barrels, Nordson EFD) was used to fill the paste
159 into the syringe cartridge in the 3D printer (regenHU 3D printer). A stopper was fixed into
160 Luer-Lock thread at the top end of the barrel after the filling process to avoid any
161 unintentional leakage of paste from the cartridge. Once ready for printing, the stopper was
162 removed, and the required nozzle (Optimum® SmoothFlow™ tapered dispensing tips, 31.24
163 mm length, Nordson EFD) was installed. The inserted piston was pushed upwards to remove
164 any trapped air in the barrels and to deliver the paste into the nozzle. The filled cartridge was
165 then installed into the printer head and the paste was extruded layer by layer until the desired
166 tablet dimension was reached. The printed tablets were left on a heated printing platform (80
167 °C) for 3 hours for complete drying (Figure 1) and (supplementary data, Appendix A, Figure
168 S.I. 1 and Table S.I. 1). The following printing parameters were used; extrusion temperature
169 was 23 °C, speed while travelling (6 mm/s) and layer height (0.40mm). The infill percentage
170 was 100% to avoid void formation inside the tablets and to produce tablets with high density.
171 Tip diameter 0.4 mm, printing pressure = 1.8 bar, number of printed layers = 14, and total
172 printing time = 8 min/tablet.

173 **1.2.2.4. Dissolution studies**

174 *In vitro* drug release studies of the paracetamol immediate release 3D printed tablets were
175 performed using a USP Type I apparatus (rotation speed at 30 rpm, 900 ml phosphate buffer,
176 pH 6.8 as the dissolution media at 37±0.5 °C). 5.0 ml samples were withdrawn at 5, 10, 15,
177 20, and 30 min. The samples were centrifuged and 0.5 ml from the supernatant was drawn
178 and diluted to 10 ml using the dissolution medium. The samples were analysed with UV–vis
179 spectrophotometer (Cary® 50 UV-vis spectrophotometer) at a λ max of 243 nm. Drug

180 dissolution studies were conducted in sextuplicate and the average of percentage of
181 cumulative drug release as a function of time was determined. The calibration curve was
182 prepared using the same dissolution medium (a phosphate buffer medium at pH 6.8) and used
183 to identify concentration of paracetamol in the unknown samples (Supplementary data,
184 Appendix A, Figure S.I. 2).

185 **1.2.3. Characterization techniques**

186 **1.2.3.1. XRPD**

187 The XRPD patterns of pure paracetamol and paracetamol immediate release formulation
188 powder (powder mixture after tablet ground into powder) were obtained at room temperature
189 using an X'Pert PRO (PANalytical, Almelo, Netherlands) setup in reflection mode using Cu
190 $K\alpha_1$ (lambda =1.54 Å) operating in Bragg– Brentano geometry. The generator voltage was set
191 to 40 kV and the current to 40 mA and the samples were scanned over 2θ range of 5° until 30°
192 in a step size of 0.026°.

193 **1.2.3.2. ATR-FTIR**

194 Infrared spectra of pure paracetamol powder and the selected excipients (CCS and PVP K25)
195 were obtained using an ATR-FTIR (Agilent Cary 630 FTIR) spectrometer.

196 **1.2.3.3. DSC**

197 DSC was used to determine and compare paracetamol melting point in its pure and mixture
198 state, and to determine possible interactions between the constituents. The DSC
199 measurements were performed on TA Instruments' DSC Q2000 coupled to Universal
200 Analysis 2000 with a thermal analyzer. DSC analysis on such drug-excipient mixtures was
201 obtained by grinding paracetamol tablets and sieving the powders (<150 μm). Accurately
202 weighed samples of 3-5 mg of the powder were placed and sealed in aluminium pans. The

203 scan was performed under nitrogen flow (50 mL/min) at a heating rate of 10° C/min from 35°
204 C to 200° C. An empty sealed aluminium pan was used as reference.

205 **1.2.3.4. Scanning electron microscopy (SEM)**

206 Variable pressure scanning electron microscopy (JEOL 6060LV, UK) was used to
207 characterize the surface morphology of the paracetamol immediate release tablets at three
208 different positions (top, cross section and bottom). The SEM images were taken at different
209 magnifications for the samples. The samples were mounted onto carbon tape stubs and
210 sputter coated with gold (Leica EM SCD005 Sputter Coater).

211 **1.2.4. Physical properties of the paracetamol immediate release 3D printed tablets**

212 **1.3.4.1. Weight test**

213 Twenty paracetamol immediate release 3D printed tablets were individually weighed and
214 their average weight calculated. The individual tablet weight deviation (%) was calculated.

215 **1.3.4.2. Breaking force**

216 Tablet breaking force is a USP test used to measure crushing strength and structural integrity
217 of tablets. Six paracetamol 3D printed tablets were randomly selected and tested for breaking
218 force using a hardness tester (Hardness tester C50, I Holland Ltd., Holland). The breaking
219 force values were recorded in N (Newton) units and the average values were calculated (Pitt
220 and Heasley, 2013).

221 **1.3.4.3. Friability**

222 Twenty paracetamol 3D printed tablets were selected randomly and the tablets were
223 accurately weighed (initial weight). The tablets were placed in a friability tester and rotated at
224 a constant speed of 25 rpm for a period of 4 min in Erweka friabilator. The tablets were
225 cleaned from loose dust and reweighed (final weight) and the weight loss % (friability)
226 calculated.

227 **1.3.4.4. Dimension of paracetamol immediate release 3D printed tablets**

228 The tablet dimension values were recorded using Vernier callipers and their average values
229 calculated.

230 **1.3.4.5. Disintegration test of the paracetamol immediate release 3D printed tablets**

231 A disintegration test was carried out on six paracetamol immediate release 3D printed tablets
232 using a disintegration tester (Copley Scientific, UK). Six tablets were placed in a basket-rack
233 composed of six tubes raised and lowered at a frequency rate between 29 and 32 cycles per
234 minute, with 1000 ml deionised water as the dissolution media at 37 ±0.5 °C. The
235 disintegration test was considered successful if all tablets were disintegrated and passed
236 through a 10-mesh screen at the bottom end of the basket-rack.

237 **1.3. Results and discussion**

238 1.3.1. **Tablet printing**

239 Batches of tablets were printed following the outlined method. Examples are shown in Figure
240 1.

241 1.3.2. ***Tablet morphology***

242 Figure 2 shows examples of the paracetamol oval tablets. There are some small lines visible
243 on the top of the tablets due to the paracetamol paste strands when printing. These lines can
244 be reduced if a tip with smaller internal diameter is used, although this increases print time.
245 Oval tablets were printed as studies have concluded that round tablets are more difficult to
246 swallow and have a slower esophageal transit times than oval tablets of the same weight
247 (Hey, Jørgensen et al. 1982, Channer and Virjee 1986). Figure 3 shows examples of the
248 microstructure of paracetamol tablets (top, cross section, and bottom).

249

250

251 1.3.3. ***In vitro* drug dissolution**

252 Dissolution data from the paracetamol 3D printed tablets show that more than 90% of the
253 paracetamol was released within the first 10 min (Figure 2). This rapid drug release is
254 attributed to the inclusion of the disintegrant sodium crosscarmellose, which rapidly absorbs
255 water and swells leading to the disintegration of the tablets. Furthermore, the formation of a
256 microporous structure (Figure 3) due to the evaporation of water from the 3D printed tablets
257 during drying also facilitated the dissolution medium penetration, fast disintegration and
258 rapid drug release.

259 **1.3.4. XRPD**

260 XRPD of the pure as-received paracetamol powder before printing, and the tablets was done
261 to investigate any changes in physical form on printing (Figures 4 and 5). The Bragg peaks
262 observed from the pure paracetamol (as received) match the Bragg peaks of paracetamol
263 (calculated) reported in the Cambridge Structural Database (CSD) (Figure 4).

264 The results in figure 5 shows that the paracetamol (non-ground and ground powder) exhibited
265 multiple sharp Bragg peaks in their XRPD patterns related to their crystalline nature. The
266 post-printing XRPD data show that the same Bragg peaks for the paracetamol were still
267 present. There was, therefore no evidence of a change in physical form (Form I) for the
268 paracetamol in this formulation fabricated using extrusion based 3D printing. As we used a
269 significant quantity of water and PVP K25 as a binder, we believe that a portion of the
270 paracetamol powder could have dissolved in the water (paracetamol solubility 12.78 g/l /20
271 °C) (Granberg and Rasmuson, 1999) as the whole mixture formed a paste, however this must
272 have recrystallised back into form I if this had occurred. XRPD also did not show evidence of
273 incompatibility between paracetamol and the chosen excipients ((PVP K25 (11.25 %) and
274 CCS (8.75 %)) in the tablets (Figure 5).

275 **1.3.5. ATR-FTIR**

276 Infrared spectral data show the characteristic peaks positions remained unchanged from the
277 paracetamol powder to the formulation, indicating that there were no detectable interactions
278 between the paracetamol and the selected excipients (PVP K25 (11.25 %) and CCS (8.75 %))
279 (Figure 6).

280 **1.3.6. DSC**

281 DSC analysis was performed to explore the stability of drug crystallinity after the 3D printing
282 process (grinding, mixing, paste formulation and drying process on a hot plat heated at 80
283 °C). DSC data shows that the pure drug powder melts at 169.7 °C confirming the presence of
284 form I (Sibik et al., 2014) while pure PVP K25 shows a glass transition around 155 °C
285 (Figure 7). The DSC data of the paracetamol formulation shows clear evidence of an
286 endothermal event (melting point) at 169.7 °C, indicating that the drug is still in a crystalline
287 form, specifically form I. This finding was also confirmed by X-ray powder diffraction data
288 (Figure 5). A further confirmation found from the SEM images of the cross sections view of
289 paracetamol sold tablets shows the presence of crystals on the surface and the SEM images
290 corroborates this extent (Fig. 3). From the above results and discussions we found that DSC
291 thermogram of paracetamol formulation powder after blending, printing, and post-printing
292 processes with the excipients; PVP K25 and NaCCS did not show significant changes in peak
293 placement apart from the peak depression and reduction caused by the presence of the
294 polymer in the formulation in comparison to the peak obtained from the pure paracetamol
295 powder and again suggesting compatibility of the excipients.

296 **1.3.7. Physical properties**

297 The 3D printed tablets were evaluated for breaking force, friability, weight variation, tablet
298 dimension, and disintegration time.

299 **1.3.7.1. Weight uniformity**

300 In quality control, oral tablets/capsules (dose and ratio of drug substance ≥25 mg and ≥25 %,
301 respectively) are required to meet the weight variation test and confirm that all
302 tablets/capsules in a batch are within the acceptable limits (Allen et al., 2011, Jatto and
303 Okhamafe, 2002). In our case the active (paracetamol) content represents the major part of
304 the tablets (80 % w/w) and therefore control of the 3D printed tablet total weight is a
305 satisfactory control for content uniformity of the drug. The paracetamol immediate release
306 3D printed tablets showed a percentage weight variation within the range of -2.17 to +1.70
307 and, therefore, comply with the USP specification for uncoated tablets (±7.5%) table 2 (Allen
308 et al., 2011, Jatto and Okhamafe, 2002).

309 **1.3.7.2. Breaking force**

310 Acceptable tablets should have sufficient strength to resist breaking and mechanical shocks
311 during transportation and storage. However, tablets also should be soft enough to disintegrate
312 properly after swallowing and releasing the drug. In a conventional tableting press, the
313 tablet's breaking force is controlled by compression forces. A tablet with a breaking force of
314 4 kg or above is considered to be satisfactory (Remington et al., 2006). In contrast, in 3D
315 printing process, the binder is essentially used to control tablet breaking force rather than
316 compression force. Examples of binders used in extrusion-based 3D printing process are
317 PVP, hydroxyl propyl methyl cellulose (HPMC), and hydro-alcoholic gels (Khaled et al.,
318 2014, Khaled et al., 2015). From the data set presented in table 3, breaking force
319 measurements were within the accepted range of 7.5-8.5 kg, and therefore, comply with USP
320 specifications. Tensile fracture strength of flat faced oval paracetamol tablets were calculated
321 using equation 1 (Stanley and Newton, 1980).

322 $\sigma_f = 3FL/2bd^2$ Eq. 1

323 Where (σ_f) is the tensile fracture strength of the tablet, (F) is the breaking force, (l) is the
324 tablet length, (b) is the tablet width and (d) is the tablet thickness.

325 **1.3.7.3. Friability**

326 This is a USP test used to determine a tablets resistance to chipping, capping, and abrasion
327 occurred during manufacturing, packaging, and shipping processes. The paracetamol
328 immediate release 3D printed tablets showed a percentage of weight loss of 0.54 % which is
329 within the range of not more than 1% of tablet weight and, therefore, the tablets again meet
330 USP specifications (Nilawar et al., 2013).

331 **1.3.7.4. Tablet size and dimension**

332 The data in Table 6 confirm that the tablet's size and dimension printed by extrusion based
333 3D printing process were reproducible and comparable with the designed tablet's size and
334 dimension and with the tablet sizes reported in the literature prepared by conventional
335 tableting machines (Brotherman et al., 2004, Channer and Virjee, 1986, Hey et al., 1982).

336 **1.3.7.5. Disintegration test**

337 Disintegration testing of oral solid dosage forms is another important physical parameter and
338 can be a key factor for a good drug bioavailability. Tablets with a fast disintegration time will
339 have a quicker dissolution time, potentially resulting in improved bioavailability. Table 5
340 shows that all the 3D printed tablets tested have a disintegration time between 57 s and 66 s
341 with an average of 61 s and that is therefore within the acceptable range of USP where 30
342 min is the maximum disintegration time for the majority of the compressed tablets
343 (Tarannum et al., 2013).

344 **1.4. Potential practice of extrusion based 3D printing process**

345 Customizing medicines for individual patients using a 3D printer is a promising application
346 that could provide new opportunities for the pharmaceutical industry and for patients. 3D

347 printers could potentially be used to print highly tailored medicines, for example with
348 deposition of different active ingredients separated with a compatible polymer could increase
349 patient compliance and reduce drug side effects and toxicity. Formulation of multi-prescribed
350 medicines into one tablet with a tailored dose and desired drug release profile can be a
351 challenging using a conventional tableting process. Hence, physicians are restricted in
352 achieving an accurate dosing regimen for a specific patient group according to patient's
353 genetic factors, body mass index (BMI) and age (Sandler et al., 2011, Voura et al., 2011).
354 Furthermore, using 3D printers could eliminate a number of steps in tablet pipeline
355 production process, such as powder milling, wet granulation, dry granulation, tablet
356 compression, coating, and long-term stability studying tests especially, when there is limited
357 quantity of active ingredients at early drug development stage (Voura et al., 2011).
358 3D printer could also play an important role in bringing the final product closer to the patient
359 through so-called distributed manufacturing. Distribution manufacturing is defined as raw
360 materials and methods of fabrications being decentralised and the final product being
361 manufactured very close to the customer (much like a compounding pharmacists would do
362 manually). This could offer a quick point of care manufacturing process and fast medicines
363 supply, producing accurate tailored dose for individuals. The schematic diagram in figure 8
364 indicates how 3D printing could provide a new method for the drug manufacturing process.
365
366
367
368
369
370
371

372 **1.5. Conclusions**

373 Extrusion based 3D printing of paracetamol immediate release tablets with a very high drug
374 loading (80 % w/w) was successfully demonstrated. The 3D printed tablets released more
375 than 90 % of the active within 10 min. XRPD, FTIR, DSC and SEM data show that the
376 paracetamol form was unaffected by the printing and that there was no detectable interactions
377 between the paracetamol and the chosen excipients (PVP K25 and CCS). The 3D printed
378 paracetamol tablets were also evaluated for weight variation, hardness, friability,
379 disintegration time, and size and dimension and were within acceptable range as defined by
380 the international standards stated in the USP. The present work is a step towards the practical
381 demonstration and validation of 3D printing of tablets with high drug loading for the tailored
382 manufacture of medicines and personalised care and treatment. The work clearly
383 demonstrates the capability of 3D extrusion based printing to produce acceptable tablets from
384 approved materials that comply with current USP standards and that if a suitable regulatory
385 and quality environment can be established that this could be achieved in a distributed
386 manufacture model.

387

388 **Acknowledgments**

389 We gratefully acknowledge GSK for the funding of this work and Dr Jing Yang for access to
390 the 3D printer. We also thank DFE Pharma for the complementary supply of CCS.

391

392

393

394

395 **1.6. References**

396 Agrawal, R., Naveen, Y., 2011. Pharmaceutical processing–A review on wet granulation
397 technology. International journal of pharmaceutical frontier research 1 (1), 65-83.

398 Allen, L.V., Popovich, N.G., Ansel, H.C., 2011. pharmaceutical dosage forms and drug
399 delivery systems Lippincott Williams & Wilkins, New York.

400 Brotherman, D.P., Bayraktaroglu, T.O., Garofalo, R.J., 2004. Comparison of ease of
401 swallowing of dietary supplement products for age-related eye disease. Journal of the
402 American Pharmacists Association 44 (5), 587-593.

403 Capes, J.S., Cameron, R.E., 2007. Contact line crystallization to obtain metastable
404 polymorphs. Crystal growth and design 7 (1), 108-112.

405 Channer, K.S., Virjee, J.P., 1986. The effect of size and shape of tablets on their esophageal
406 transit. The Journal of Clinical Pharmacology 26 (2), 141-146.

407 Clark, E.A., Alexander, M.R., Irvine, D.J., Roberts, C.J., Wallace, M.J., Sharpe, S., Yoo, J.,
408 Hague, R.J.M., Tuck, C.J., Wildman, R.D., 2017. 3D printing of tablets using inkjet with UV
409 photoinitiation. International Journal of Pharmaceutics 529 (1), 523-530.

410 Di Martino, P., Conflant, P., Drache, M., Huvenne, J.-P., Guyot-Hermann, A.-M., 1997.
411 Preparation and physical characterization of forms II and III of paracetamol. Journal of
412 Thermal Analysis and Calorimetry 48 (3), 447-458.

413 Di Martino, P., Guyot-Hermann, A.M., Conflant, P., Drache, M., Guyot, J.C., 1996. A new
414 pure paracetamol for direct compression: The orthorhombic form. International Journal of
415 Pharmaceutics 128 (1), 1-8.

416 Eichie, F., Amalime, A., 2007. Evaluation of the binder effects of the gum mucilages of
417 Cissus populnea and Acassia senegal on the mechanical properties of paracetamol tablets.
418 African Journal of Biotechnology 6 (19).

419 Fachaux, J.M., Guyot-Hermann, A.M., Guyot, J.C., Conflant, P., Drache, M., Veesler, S.,
420 Boistelle, R., 1995. Pure Paracetamol for direct compression Part I. Development of sintered-
421 like crystals of Paracetamol. Powder Technology 82 (2), 123-128.

422 Gohel, M.C., Jogani, P.D., 2005. A review of co-processed directly compressible excipients.
423 Journal of Pharmacy and Pharmaceutical Sciences 8 (1), 76-93.

424 Govedarica, B., Injac, R., Srcic, S., 2009. Formulation and evaluation of immediate release
425 tablets with different types of paracetamol powders prepared by direct compression. African
426 Journal of Pharmacy and Pharmacology 5 (1), 31-41.

427 Goyanes, A., Buanz, A.B.M., Hatton, G.B., Gaisford, S., Basit, A.W., 2015. 3D printing of
428 modified-release aminosalicylate (4-ASA and 5-ASA) tablets. European Journal of
429 Pharmaceutics and Biopharmaceutics 89, 157-162.

430 Goyanes, A., Fina, F., Martorana, A., Sedough, D., Gaisford, S., Basit, A.W., 2017.
431 Development of modified release 3D printed tablets (printlets) with pharmaceutical
432 excipients using additive manufacturing. International Journal of Pharmaceutics 527 (1–2),
433 21-30.

434 Goyanes, A., Kobayashi, M., Martínez-Pacheco, R., Gaisford, S., Basit, A.W., 2016. Fused-
435 filament 3D printing of drug products: Microstructure analysis and drug release
436 characteristics of PVA-based caplets. International Journal of Pharmaceutics 514 (1), 290-
437 295.

438 Granberg, R.A., Rasmuson, Å.C., 1999. Solubility of Paracetamol in Pure Solvents. Journal
439 of Chemical & Engineering Data 44 (6), 1391-1395.

440 Hey, H., Jørgensen, F., Sørensen, K., Hasselbalch, H., Wamberg, T., 1982. Oesophageal
441 transit of six commonly used tablets and capsules. British Medical Journal (Clinical research
442 ed.) 285 (6356), 1717-1719.

443 Holländer, J., Genina, N., Jukarainen, H., Khajeheian, M., Rosling, A., Mäkilä, E., Sandler,
444 N., 2016. Three-dimensional printed PCL-based implantable prototypes of medical devices
445 for controlled drug delivery. Journal of Pharmaceutical Sciences 105 (9), 2665-2676.

446 Jatto, E., Okhamafe, A.O., 2002. An overview of pharmaceutical validation and process
447 controls in drug development. Tropical Journal of Pharmaceutical Research 1, 116-117.

448 Kaerger, J.S., Edge, S., Price, R., 2004. Influence of particle size and shape on flowability
449 and compactibility of binary mixtures of paracetamol and microcrystalline cellulose.
450 European Journal of Pharmaceutical Sciences 22 (2–3), 173-179.

451 Karki, S., Friščić, T., Fábián, L., Laity, P.R., Day, G.M., Jones, W., 2009. Improving
452 mechanical properties of crystalline solids by cocrystal formation: new compressible forms of
453 paracetamol. Advanced Materials 21 (38□39), 3905-3909.

454 Katstra, W.E., Palazzolo, R.D., Rowe, C.W., Giritlioglu, B., Teung, P., Cima, M.J., 2000.
455 Oral dosage forms fabricated by three dimensional printing™. Journal of Controlled Release
456 66 (1), 1-9.

457 Khaled, S.A., Burley, J.C., Alexander, M.R., Roberts, C.J., 2014. Desktop 3D printing of
458 controlled release pharmaceutical bilayer tablets. International Journal of Pharmaceutics 461
459 (1–2), 105-111.

460 Khaled, S.A., Burley, J.C., Alexander, M.R., Yang, J., Roberts, C.J., 2015. 3D printing of
461 five-in-one dose combination polypill with defined immediate and sustained release profiles.
462 Journal of Controlled Release 217, 308-314.

463 Khaled, S.A., Burley, J.C., Alexander, M.R., Yang, J., Roberts, C.J., 2015. 3D printing of
464 tablets containing multiple drugs with defined release profiles. International Journal of
465 Pharmaceutics 494 (2), 643-650.

466 Kyobula, M., Adedeji, A., Alexander, M.R., Saleh, E., Wildman, R., Ashcroft, I., Gellert,
467 P.R., Roberts, C.J., 2017. 3D inkjet printing of tablets exploiting bespoke complex
468 geometries for controlled and tuneable drug release. Journal of Controlled Release 261
469 (Supplement C), 207-215.

470 Martinello, T., Kaneko, T.M., Velasco, M.V.R., Taqueda, M.E.S., Consiglieri, V.O., 2006.
471 Optimization of poorly compactable drug tablets manufactured by direct compression using
472 the mixture experimental design. International Journal of Pharmaceutics 322 (1), 87-95.

473 Ngwuluka, N., Idiakhoa, B., Nep, E., Ogaji, I., Okafor, I., 2010. Formulation and evaluation
474 of paracetamol tablets manufactured using the dried fruit of Phoenix dactylifera Linn as an
475 excipient. Research in Pharmaceutical Biotechnology 2 (3), 025-032.

476 Nichols, G., Frampton, C.S., 1998. Physicochemical characterization of the orthorhombic
477 polymorph of paracetamol crystallized from solution. Journal of Pharmaceutical Sciences 87
478 (6), 684-693.

479 Nilawar, P.S., Wankhade, V., Badnag, D., 2013. An emerging trend on bilayer tablets.
480 International Journal of Pharmacy and Pharmaceutical Science Research 3 (1), 15-21.

481 Okwuosa, T.C., Stefaniak, D., Arafat, B., Isreb, A., Wan, K.W., Alhnan, M.A., 2016. A
482 Lower Temperature FDM 3D Printing for the Manufacture of Patient-Specific Immediate
483 Release Tablets. Pharm Res 33 (11), 2704-2712.

484 Pietrzak, K., Isreb, A., Alhnan, M.A., 2015. A flexible-dose dispenser for immediate and
485 extended release 3D printed tablets. Eur J Pharm Biopharm 96, 380-387.

486 Pitt, K.G., Heasley, M.G., 2013. Determination of the tensile strength of elongated tablets.
487 Powder Technology 238, 169-175.

488 Rattanakit, P., Moulton, S.E., Santiago, K.S., Liawruangrath, S., Wallace, G.G., 2012.
489 Extrusion printed polymer structures: A facile and versatile approach to tailored drug delivery
490 platforms. International Journal of Pharmaceutics 422 (1–2), 254-263.

491 Remington, J.P., Troy, D.B., Beringer, P., 2006. Remington: the science and practice of
492 pharmacy. Lippincott Williams & Wilkins.

493 Rowe, C.W., Katstra, W.E., Palazzolo, R.D., Giritlioglu, B., Teung, P., Cima, M.J., 2000.
494 Multimechanism oral dosage forms fabricated by three dimensional printing™. Journal of
495 Controlled Release 66 (1), 11-17.

496 Sandler, N., Määttänen, A., Ihalainen, P., Kronberg, L., Meierjohann, A., Viitala, T.,
497 Peltonen, J., 2011. Inkjet printing of drug substances and use of porous substrates-towards
498 individualized dosing. *Journal of Pharmaceutical Sciences* 100, 3386-3395.

499 Sibik, J., Sargent, M.J., Franklin, M., Zeitler, J.A., 2014. Crystallization and phase changes in
500 paracetamol from the amorphous solid to the liquid phase. Molecular Pharmaceutics 11 (4),
501 1326-1334.

502 Skowyra, J., Pietrzak, K., Alhnan, M.A., 2015. Fabrication of extended-release patient-
503 tailored prednisolone tablets via fused deposition modelling (FDM) 3D printing. European
504 Journal of Pharmaceutical Sciences 68, 11-17.

505 Stanley, P., Newton, J., 1980. The tensile fracture stress of capsule□shaped tablets. Journal
506 of Pharmacy and Pharmacology 32 (1), 852-854.

507 Sun, Y., Soh, S., 2015. Printing tablets with fully customizable release profiles for
508 personalized medicine. Advanced Materials 27 (47), 7847-7853.

509 Tarannum, A., Shamsi, S., Zaman, R., 2013. Development of standard operating procedures
510 of Habbe Shifa: A polyherbal Unani formulation. Journal of Ayurveda and Integrative
511 Medicine 4 (3), 147-151.

512 Voura, C., Gruber, M., Schroedl, N., Strohmeier, D., Eitzinger, B., Bauer, W., Brenn, G.,
513 Khinast, J., Zimmer, A., 2011. Printable medicines: a microdosing device for producing
514 personalised medicines. *Pharmaceutical Technology Europe* 23, 32-36.

515 Wang, J., Goyanes, A., Gaisford, S., Basit, A.W., 2016. Stereolithographic (SLA) 3D printing
516 of oral modified-release dosage forms. International Journal of Pharmaceutics 503 (1–2),
517 207-212.

518 Whittaker, C., 2011. Over-the-counter pain management guidelines: primary health care.
519 Professional Nursing Today 15 (1), 16-20.

520 Wu, C.-Y., Hancock, B., Mills, A., Bentham, A., Best, S., Elliott, J., 2008. Numerical and
521 experimental investigation of capping mechanisms during pharmaceutical tablet compaction.
522 Powder Technology 181 (2), 121-129.

523

524 # Captions of figures

525 Figure 1: Photographs of paracetamol immediate release tablets.

526 Figure 2: *In vitro* cumulative drug release profile of paracetamol immediate release tablets.
527 14.7mm length × 7.5 mm width × 5.0 mm height (average, n = 6).

528 Figure 3: SEM micrograph of paracetamol immediate release 3D tablets (top, cross section,
529 and bottom).

530 Figure 4: XRPD patterns of the calculated (top) and reference (measured) paracetamol.

531 Figure 5: XRPD patterns of paracetamol powder (non-ground and ground Form I) (left),
532 paracetamol powder (ground Form I), paracetamol formulation, PVP K25, CCS and Brass
533 (sample holder) (right).

534 Figure 6: FTIR spectra of paracetamol powder (ground Form I) and paracetamol formulation
535 (right), PVP K25, CCS (left).

536 Figure 7: DSC thermograms of pure paracetamol, paracetamol formulation, PVP K25, and
537 NaCCS.

538 Figure 8: Schematic diagram represents how application of 3D printing in manufacturing
539 distribution could change the drug manufacturing process.

540

541

542

543

544

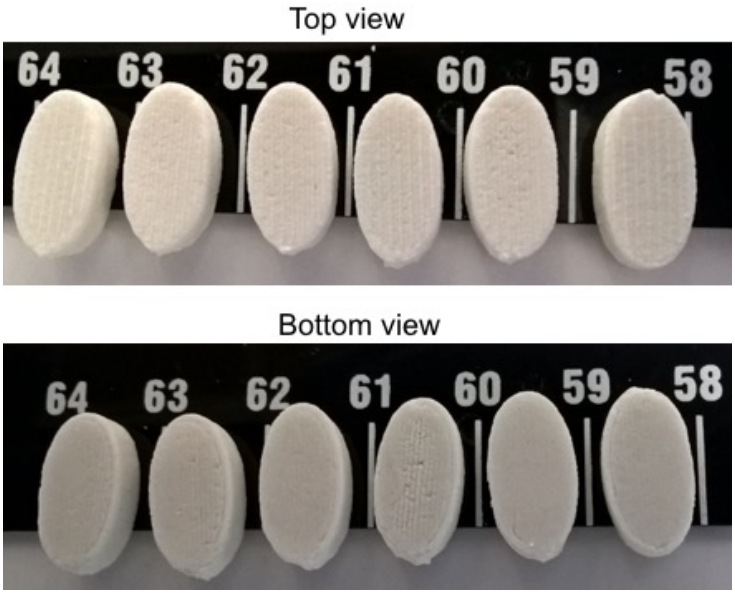

Figure 1: Photographs of paracetamol immediate release tablets.

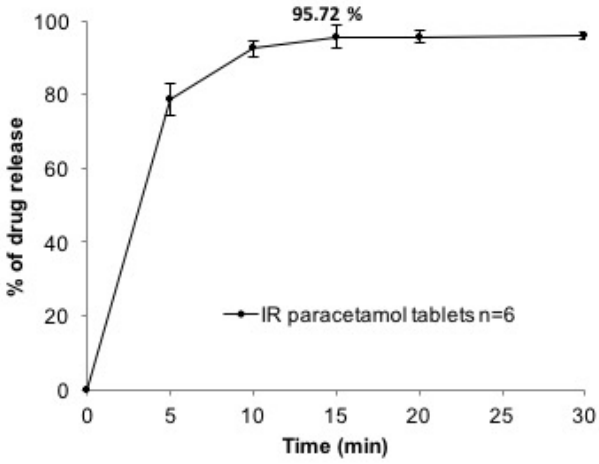

Figure 2: *In vitro* cumulative drug release profile of paracetamol immediate release tablets. 14.7mm length × 7.5 mm width × 5.0 mm height (average, n = 6).

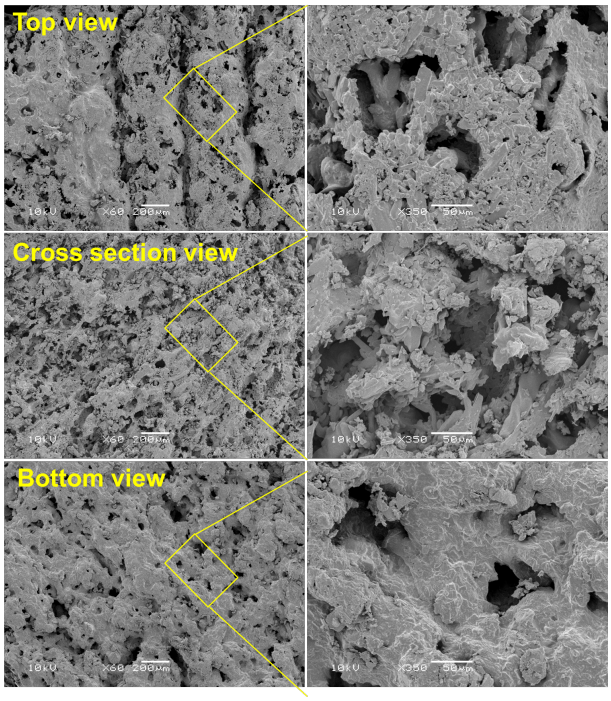

Figure 3: SEM micrograph of paracetamol immediate release 3D tablets (top, cross section, and bottom).

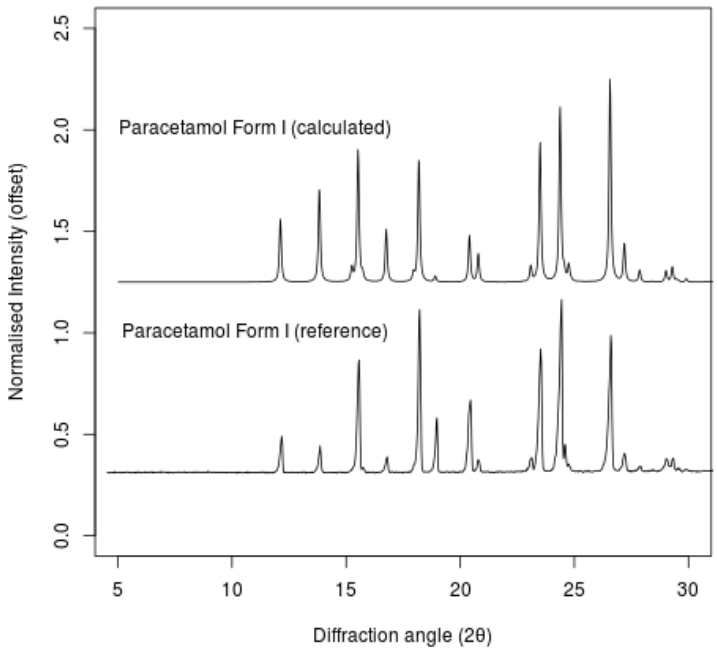

Figure 4: XRPD patterns of the calculated (top) and reference (measured) paracetamol.

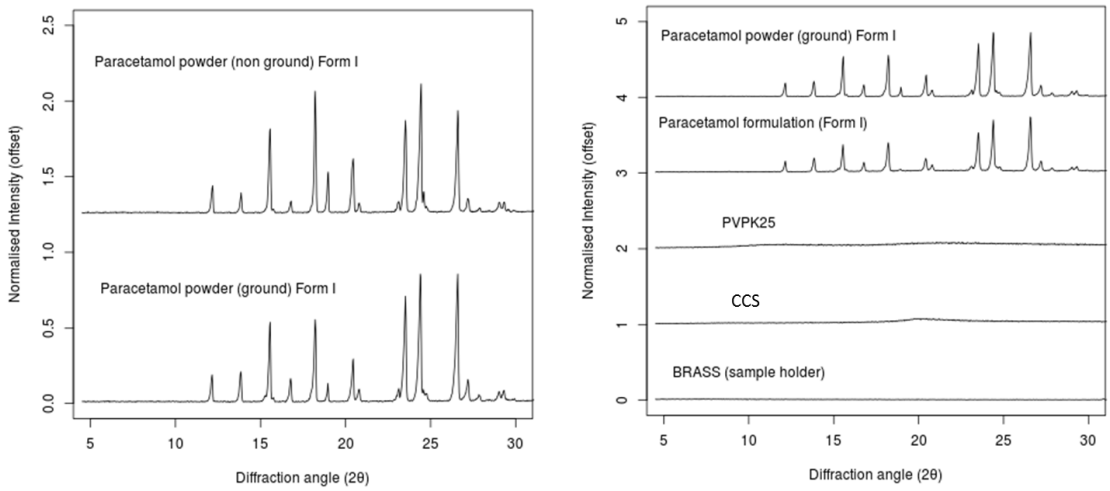

557

558 Figure 5: XRPD patterns of paracetamol powder (non-ground and ground Form I) (left), paracetamol

559 powder (ground Form I), paracetamol formulation, PVP K25, CCS and Brass (sample holder) (right).

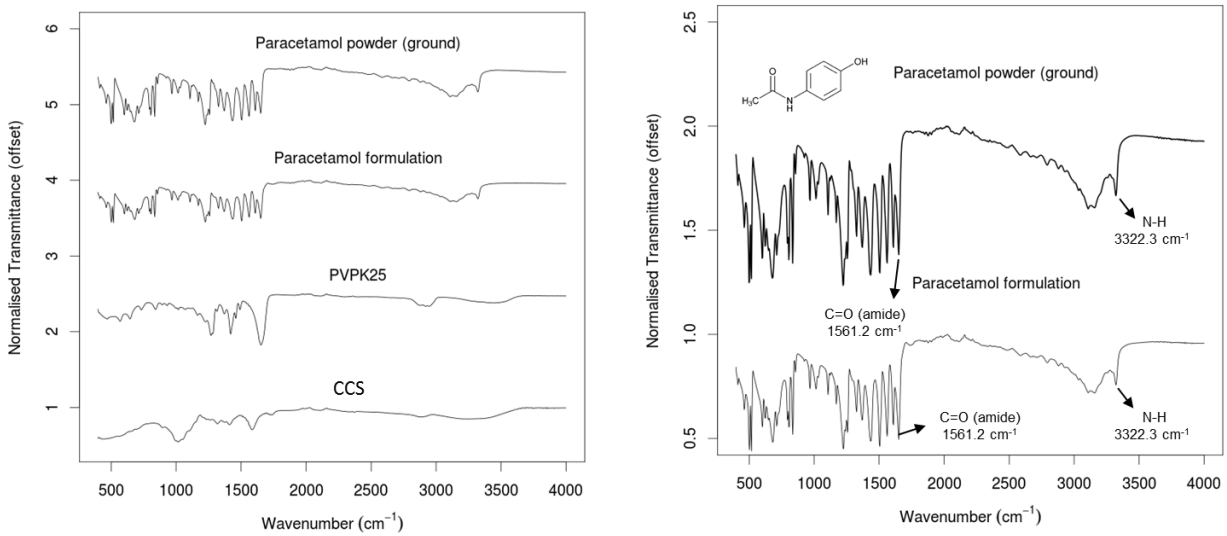

560

561 Figure 6: FTIR spectra of paracetamol powder (ground Form I) and paracetamol formulation (left),

562 PVP K25, CCS (right).

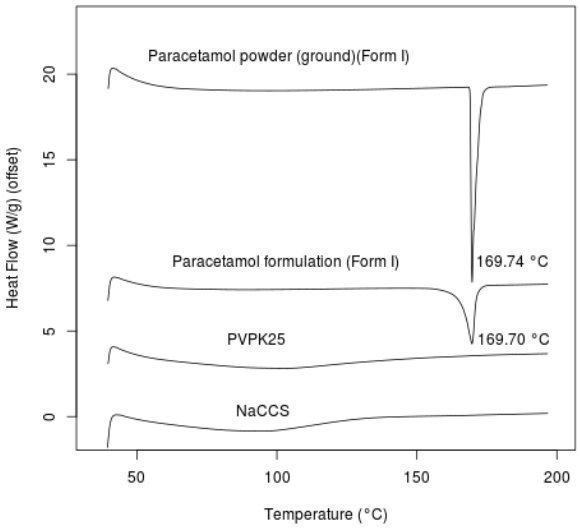

Figure 7: DSC thermograms of pure paracetamol, paracetamol formulation, PVP K25, and NaCCS.

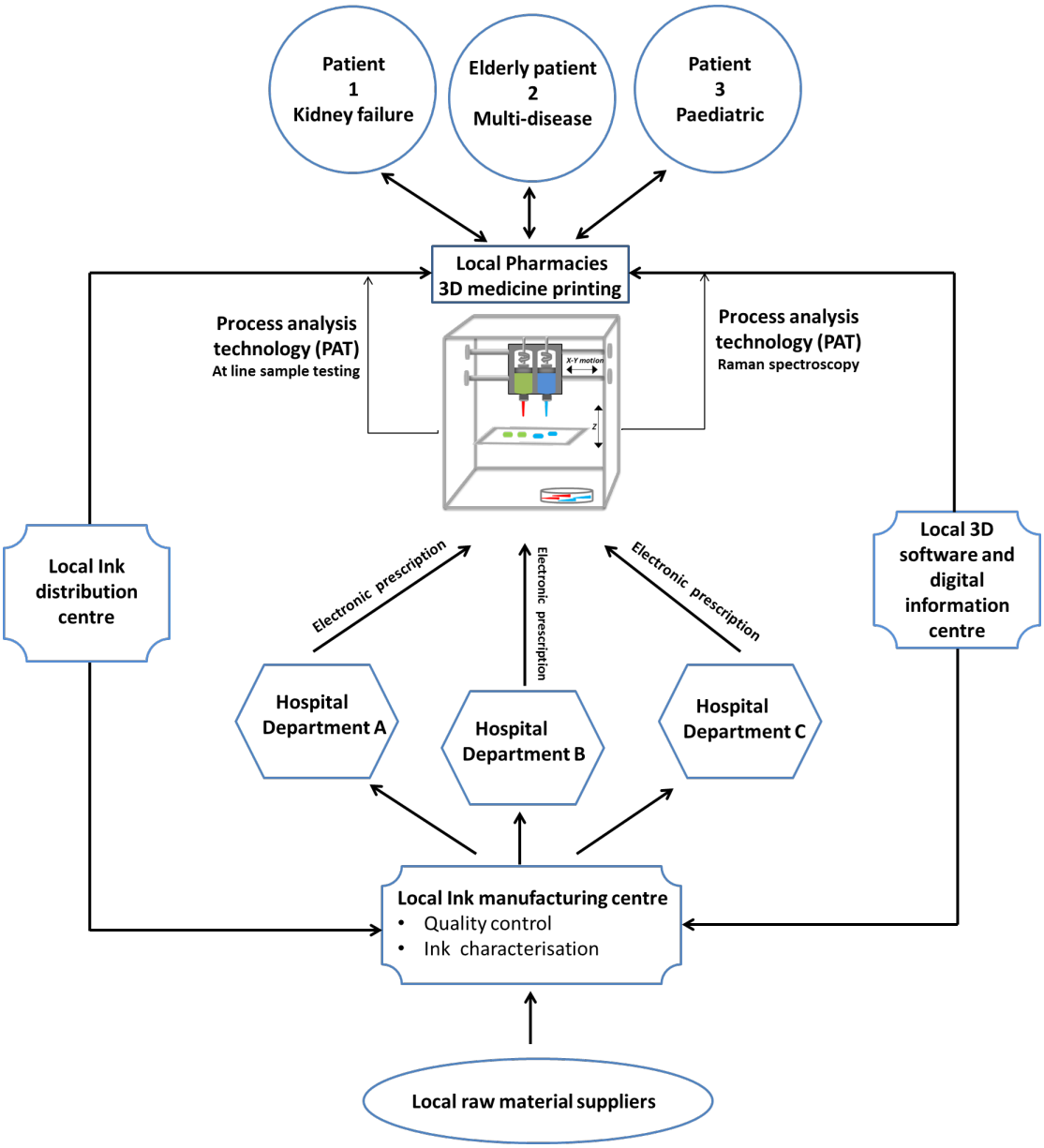

Figure 8: Schematic diagram represents how application of 3D printing in manufacturing distribution could change the drug manufacturing process.

578 # Tables

579 Table 1: The percentage composition of various ingredients in paracetamol immediate release
580 formulation feed stock.

Name of Comp.	Function	Total formulae (mg)	Dry formulae (wt. % w/w)	Wet formulae (wt. % w/w)	Dry tablets* (mg)
Paracetamol	API**	800	80	48.49	254.72
PVP	Binder	112.5	11.25	6.82	35.82
NaCCS	Disintegrant	87.5	8.75	5.30	27.86
Water	Binder	650	---	39.40	---

581 * Calculated from the average of the total paracetamol tablet weight (318.4 mg), ** Active
582 Pharmaceutical Ingredient

583 Table 2: Individual paracetamol immediate release 3D printed tablets weight, percentage
584 deviation, and their average, median, maximum, minimum weight and standard deviation.

Tablet no.	Tablet weight (mg)	Deviation %
1	322.80	1.70
2	314.20	-1.01
3	316.90	-0.15
4	320.90	1.11
5	320.50	0.98
6	319.50	0.66
7	318.50	0.35
8	310.50	-2.17
9	315.70	-0.53
10	321.70	1.36
11	318.80	0.44
12	311.80	-1.76
13	318.80	0.44
14	322.30	1.55
15	310.80	-2.08
16	312.00	-1.70
17	316.80	-0.19
18	320.00	0.82
19	315.00	-0.75
20	320.30	0.92

Average	317.39	0.00
Median	318.65	0.40
Maximum	322.80	1.70
Minmum	310.50	-2.17
SD ±	3.80	1.20

585

586 Table 3: Individual paracetamol immediate release 3D printed tablets breaking force (N),
587 tensile fracture strength (MPa), and their average, median, maximum, minimum hardness and
588 standard deviation.

Tablet no.	Breaking force (kg)	Breaking force (N)	Tensile strength (MPa)
1	8.20	80.40	9.65
2	7.72	75.70	9.00
3	8.49	83.30	9.54
4	7.50	73.60	8.32
5	8.03	78.80	8.67
6	7.85	77.00	8.40
Average	7.97	78.13	8.93
Median	7.94	77.90	8.84
Maximum	8.49	83.30	9.65
Minimum	7.50	73.60	8.32
SD ±	0.32	3.16	0.52

589

590 Table 4: Individual immediate release paracetamol 3D printed tablets dimension and their
591 average, median, maximum, minimum dimension, standard deviation.

Dimension (mm)	Tablet 1	Tablet 2	Tablet 3	Tablet 4	Tablet 5	Tablet 6	Average (mm)	Median (mm)	Maximum (mm)	Minimum (mm)	SD (±)
Length	14.52	14.51	14.45	14.44	14.59	14.58	14.52	14.52	14.68	14.44	0.0
Width	7.53	7.59	7.48	7.51	7.53	7.47	7.52	7.52	7.59	7.47	0.04
Thickness	4.91	4.91	5.03	5.05	5.14	5.18	5.04	5.04	5.18	4.91	0.10

592

593 Table 5: Disintegration time of paracetamol 3D printed tablets.

Tab No.	Disintegration time (Sec.)
1	66
2	60
3	59
4	60

5	57
6	65
Average	61
Median	60
Maximum	66
Minimum	57
SD ±	4

Supplementary information (Appendix A)

Captions of figures

S. I. Figure 1: Loss on drying data shows total weight of paracetamol immediate release 3D printed tablets (placed on a hot plate at a fixed temperature 80 °C) as function of time

S. I. Figure 2: Calibration curve of paracetamol in phosphate buffer medium at pH 6.8.

Tables

S. I. Table 1: Loss on drying data shows total weight of paracetamol immediate release 3D printed tablets (placed on a hot plate at a fixed temperature 80 °C) as function of time.

Time (hrs)	**Tablet total wt. (mg)**			
	Tablet 1	Tablet 2	Tablet 3	Average wt.
01:00	395.5	393.1	394.2	394.3
01:15	377.7	378.4	380.2	378.8
01:30	370.3	365.2	366.5	367.3
01:45	358.9	354.1	356.4	356.5
02:00	348.2	343.9	345.7	345.9

02:15	339.1	335.7	335	336.6
02:30	332.4	328.8	331	330.7
02:45	327.1	325	326.8	326.3
03:00	**323.8**	**323.5**	**324**	**323.8**
03:15	**322.7**	**322.4**	**323.8**	**322.6**
03:30	**322.6**	**322.3**	**322.4**	**322.4**

605